Published in final edited form as:
Nat Struct Mol Biol. 2015 September ; 22(9): 686–694. doi:10.1038/nsmb.3070.

Probing $G\alpha_{i1}$ Protein Activation at Single Amino Acid Resolution

Dawei Sun[1,2], **Tilman Flock**[#3], **Xavier Deupi**[#1,4], **Shoji Maeda**[1,6], **Milos Matkovic**[1,2], **Sandro Mendieta**[1], **Daniel Mayer**[1,2], **Roger Dawson**[5], **Gebhard F.X. Schertler**[1,2], **M. Madan Babu**[3], and **Dmitry B. Veprintsev**[1,2]

[1]Laboratory of Biomolecular Research, Paul Scherrer Institute, Villigen, Switzerland [2]Department of Biology, Swiss Federal Institute of Technology Zurich, Zurich, Switzerland [3]Medical Research Council Laboratory of Molecular Biology, Cambridge, United Kingdom [4]Condensed Matter Theory Group, Paul Scherrer Institut, Villigen, Switzerland [5]F. Hoffmann-La Roche AG, Pharma Research & Early Development, Discovery Technologies, Basel, Switzerland

[#] These authors contributed equally to this work.

Abstract

We present comprehensive single amino acid resolution maps of the residues stabilising the human $G\alpha_{i1}$ subunit in nucleotide- and receptor-bound states. We generated these maps by measuring the effects of alanine mutations on the stability of $G\alpha_{i1}$ and of the rhodopsin-$G\alpha_{i1}$ complex. We identified stabilization clusters in the GTPase and helical domains responsible for structural integrity and the conformational changes associated with activation. In activation cluster I, helices α1 and α5 pack against strands β1-3 to stabilize the nucleotide-bound states. In the receptor-bound state, these interactions are replaced by interactions between α5 and strands β4-6. Key residues in this cluster are Y320, crucial for the stabilization of the receptor-bound state, and F336, which stabilizes nucleotide-bound states. Destabilization of helix α1, caused by rearrangement of this activation cluster, leads to the weakening of the inter-domain interface and release of GDP.

Introduction

G protein coupled receptors (GPCRs) turn extracellular signals into intracellular responses by activating heterotrimeric G proteins 1–3. Upon binding an activating ligand, receptors catalyse the release of GDP bound to the Gα subunit. Subsequent binding of GTP causes dissociation of the Gα and Gβγ subunits from the receptor. A large number of mutagenesis studies proposed the C-terminal helix α5 of Gα as a key interaction site for receptor binding and as a conduit for signal transduction 4–9. These data, in combination with crystal structures of individual G protein subunits and of trimetric G proteins provided a broad

Correspondence should be addressed to D.B.V., dmitry.veprintsev@psi.ch.
[6]current address: Department of Molecular and Cellular Physiology, Stanford University, Stanford, USA

Author Contributions

DS collected and performed all data analysis. TF helped with analysis and interpretation. SMaeda, SMendieta and DM helped with experiments. XD built the molecular models, and MM helped with the interpretation of the structural effects of mutations. RD, GFXS and MMB contributed to the discussion and writing the manuscript. DS, XD and DBV wrote the manuscript. All authors read and provided their comments on the draft. DS and DBV conceived research and DBV supervised the project.

understanding of the G protein activation mechanism 2,10–15. More recently, the crystal structure of the β2 adrenergic receptor-Gs complex (β_2AR-Gs) 16 confirmed that the main site of interaction between the receptor and the G protein is the C-terminus of helix α5, and revealed additional contacts between intracellular loop 2 (ICL2) of the receptor and helix αN of the $G\alpha_s$. The largest conformational change in the GTPase domain was a rotation of helix α5 and its displacement towards the receptor, accompanied by rearrangements of the α5-β6 interface, the phosphate binding β1-α1 loop (P-loop) and helix α1. This structure also showed the dissociation between the GTPase and helical domains of the G protein, consistent with previous BRET, DEER and single particle electron microscopy data 17–19. Furthermore, analysis of hydrogen–deuterium exchange mass spectrometry data 20 has led to suggest that G protein activation is also associated with an increased disorder around the β1 strand and the nucleotide binding pocket, especially the P-loop and the adjacent N-terminal part of helix α5, while the C-terminus of Gα was protected upon binding the receptor.

A recent modelling study 21 has suggested that G protein activation is associated with the rearrangement of the interfaces between helices α1 and α5, and between α5 and the loop α5-β6. Subsequent experimental mutagenesis studies 22 pinpointed residue F336 in helix α5 of $G\alpha_{i1}$ as a particularly important for G protein activation, as its mutation increases the rate of spontaneous GDP release. The proposed mechanism involves F336 acting as a relay, transmitting conformational changes via strands β2, β3 and helix α1 to the phosphate binding loop.

These combined data suggest a mechanism that involves binding of the C terminus of Gα to the receptor accompanied by the formation of additional interactions between the helix αN and the receptor, and transmission of the allosteric signal via the strand β1 or via β2, β3 and helix α1 to destabilize the nucleotide binding site. However, the exact details of the molecular mechanism of the activation remain unclear.

Here, we set out to establish a detailed and comprehensive understanding of the G protein activation mechanism at the residue level that consolidates and extends the existing knowledge. To do this, we characterized the influence of each amino acid of $G\alpha_{i1}$ on the stability of the GDP- and GTP-bound states of $G\alpha_{i1}$ alone, and of the signaling complex between heterotrimeric G_i ($G\alpha_{i1}\beta_1\gamma_1$) and rhodopsin (Rho), a prototypical GPCR. The aggregated analysis of these data allowed us to draw a complete functional map of the $G\alpha_{i1}$ subunit stability at different stages of its activation cycle that allowed us to propose an activation mechanism at single amino acid resolution.

Results

We have recently showed that the complex between the heterotrimeric G_i ($G\alpha_{i1}\beta_1\gamma_1$) and rhodopsin (Rho) is more stable than the native Rho-G_t complex and is suitable for biophysical studies23. In this work we mutated each amino acid of $G\alpha_{i1}$ to alanine or glycine and quantified 1) the thermal stability of each mutant in the inactive GDP-bound and the active GTP(GTPγS)-bound states (Fig. 1 & 2, Supplementary Fig. S1, Supplementary Table 1, methods); and 2) the efficiency of formation (relative abundance) and relative

stability of the reconstituted Rho-G_i protein complex (Fig. 1, Supplementary Fig. S2, S3, S4, Supplementary Table 1, methods).

Interpretation of the changes in stability upon mutation

Mutation of an amino acid to alanine (or, to glycine, if the original amino acid is alanine) results in the elimination of the side chain, which leads to an alteration of the local structure that changes the stability of a protein or complex. If this mutation has a large effect on protein stability, this suggests that the side chain was involved in many local interactions, indicating a structured environment. Conversely, a small change in stability implies that the side chain is not involved in many local interactions. Thus, if point mutations along a stretch of residues do not affect protein stability, this region is likely to be unstructured.

Importantly, changes in protein stability are sensitive to conformational rearrangements. This is the basis of phi-value analysis, a technique developed by Alan Fersht and colleagues to study the energetic and structural details of protein folding intermediates 24. Here, we have adapted this method to study conformational changes of G_i in the GTP-bound and Rho*-G_i (where Rho* denotes light-activated state of rhodopsin) complex relative to G_i in the GDP-bound state, which we used as a reference state.

Comparison of the effects of mutations on stability for several conformational states of the protein substantially increases the “interrogating” power of the alanine scanning technique. Importantly, this technique requires a wide coverage of the protein sequence, ideally approaching 100% of mutated residues. Through the integration of this exhaustive data set, we generated a detailed interpretation of the conformational changes during protein activation, which allowed us to expand, test, or rule out existing hypothesis on the activation mechanism of G proteins.

These simple considerations formed the basis for interpreting the measured stability changes in structural terms. For instance, we found that many mutations (30-50%) destabilize both GDP-bound $G\alpha_{i1}$ and the Rho*-G_i complex (Fig. 1 & 2, Supplementary Table 1). These residues are located in regions with the same local environment (i.e. conformation) in both states, and are thus important for the stability and integrity of the protein. However, mutations at several positions have different effects on GDP-bound $G\alpha_{i1}$ and the Rho*-G_i complex, indicating that they are in regions that undergo conformational changes upon formation of the complex. This way we identified positions that contributed specifically to the stability of $G\alpha_{i1}$ in each conformation (Fig. 3).

In order to compare and extrapolate our findings to other Gα proteins, throughout this paper we used the common G protein numbering system (CGN) proposed in Flock et al.25 In this system, the superscript next to the residue number denotes: i) either the GTPase (G) or helical (H) domain, ii) the secondary structure element within each domain (e.g. HN for helix N or S1 for beta sheet β1), and iii) its position within this structural element (e.g. 1), according to a sequence alignment of 973 G protein sequences. For example, $L353^{G.H5.25}$ corresponds to the L353 in Ga_{i1}, GTPase domain, helix 5, and position 25 of the helix 5 in the universal alignment.

Europe PMC Funders Author Manuscripts

N- and C-termini become ordered in the Rho*-G_i complex

The N-terminus provided an excellent benchmark to test the capabilities of our method. Mutations at positions $1^{G.HN.8}$ to $32^{G.HNS1.3}$ had little impact on the stability of $G\alpha_{i1}$ alone, suggesting that this region was unstructured in the absence of the $G\beta\gamma$ subunit. However, mutations of the residues that form the interface with $G\beta\gamma$ in the G protein trimer (e.g., $L5A^{G.HN.12}$, $S16A^{G.HN.40}$, $I19A^{G.HN.43}$, $D20A^{G.HN.44}$ and $L23A^{G.HN.47}$) had a severe impact on the stability of the Rho*-G_i complex, while mutation of the residues in this region facing the solvent did not have such effect (Fig 1, Supplementary Table 1).

Mutation of $R32^{G.HNS1.3}$ at the base of the N-terminus stabilized the Rho*-G_i complex, most likely by improving its interactions with intracellular loop 2 (ICL2) of the receptor. This stabilization effect is probably receptor specific and thus may contribute to receptor-G protein specificity. It is also possible that this position is interacting with the helical domain in its most “open” conformation as shown in Fig 1b.

Numerous studies have shown that the last eleven residues in the C-terminus of Gα play a critical role in receptor binding8,9,26,27. Accordingly, most alanine mutations at positions $344^{G.H5.16}$-$354^{G.H5.26}$ considerably affected the formation of the Rho*-G_i complex (Fig. 1 & 4). Particularly, substitution of the conserved $L348^{G.H5.20}$ and $L353^{G.H5.25}$ and the less conserved $G352^{G.H5.24}$ at the end of the C-terminus severely impaired coupling with the receptor without affecting the stability of the nucleotide-bound states. These data agreed with NMR and crystallography studies on a G_t C-terminal peptide bound to rhodopsin, and with the crystal structure of the β_2AR-G_s complex, which showed that the C-terminus of $G\alpha_s$ becomes helical and penetrates into a crevice formed in the cytoplasmic side of the transmembrane bundle upon receptor activation 16,20,28,29. Interestingly, $N347A^{G.H5.19}$ did not affect the formation and stability of the Rho*-G_i complex, and $D350A^{G.H5.22}$ even slightly stabilized it (Fig. 4a), showing that not all amino acids in the C-terminus have the same effect on receptor binding. Finally, the absence of a destabilizing effect upon mutating positions $344^{G.H5.16}$-$354^{G.H5.26}$ in the nucleotide bound states strongly suggested that this region was unstructured in the absence of the receptor.

Rearrangement of activation cluster I upon complex formation

The movement of helix α5 in the GTPase domain upon formation of the complex 4,16,21 results in significant conformational changes around its base, which is packed against the β sheet consisting of strands β1-β6, and helix α1. Our data are in agreement with such rearrangements, as shown by the different effect of mutations on the nucleotide-bound state and on the complex. Importantly, our analysis allowed us to focus on the individual contribution to the stability of the different $G\alpha_{i1}$ states of each amino acid of this entire region. We detected a number of residues with a concerted role, which we termed as activation cluster I (Fig 3 and 5a), formed by several highly conserved hydrophobic residues from β1-3 strands, helix α1 and inward-facing residues of helix α5. Alanine substitutions of these residues considerably destabilized the GDP-bound conformation (3-18 ºC) and moderately affected the GTPγS-bound state (1-5 ºC) (Fig. 5a & 6a, Supplementary Fig. S5a, Supplementary Table 1). Importantly, mutation of $F336^{G.H5.8}$ (universally conserved in Gα

subfamilies; see Flock et al25) in helix α5 is the only substitution that resulted in a complete impairment of $G\alpha_{i1}$ stability and of its ability to bind nucleotides. F336A$^{G.H5.8}$ also caused protein aggregation and a severe impairment in reconstitution of $G\alpha_{i1}$ with Gβγ to form the Gαβγ heterotrimer (Supplementary Fig. S6). Interestingly, this mutant still formed a relatively stable complex with the receptor. In the structure of the β_2AR-G_s complex, the corresponding phenylalanine moved from the buried hydrophobic core of Gs_α to contact ICL2 of the receptor16. This suggests that F336$^{G.H5.8}$ plays a critical role in stabilizing the $G\alpha_{i1}$ subunit in the nucleotide-bound conformation, consistent with the observation that its mutation increases the rate of spontaneous nucleotide release22. We hypothesized that relocation of F336$^{G.H5.8}$ concomitant with the upward movement and twist of α5 triggers the reorganization of the cluster I into the receptor-bound state.

Upon binding the receptor, a structural reorganization of cluster I disrupts the interactions that stabilize helix α1 (Fig. 5a). This is suggested by the fact that mutation of residues I49$^{G.H1.4}$, M53$^{G.H1.8}$, and I56$^{G.H1.11}$ in α1, L38$^{G.S1.6}$ of β1, T329$^{G.H5.1}$ and V332$^{G.H5.4}$ of α5, which tether helix α1 in the $G\alpha_{i1}$-GDP state, severely impaired its stability, but did not affect the stability of Rho*-G_i complex (Fig. 6a, Supplementary Table 1). Moreover, mutation of the conserved N331$^{G.H5.3}$ and V332$^{G.H5.4}$ in helix α5, which stabilizes the nucleotide-bound state by making connections to the helix α1, increased the stability of the complex by 30% and 20%, respectively. Movement of these residues disrupted contacts between the base of helix α5 and helix α1, which would lead to the loss of helicity at the base of helix α5 observed in the β_2AR-G_s complex 16. This order-to-disorder transition potentially increased the flexibility of the loop β6-α5, which contains the guanine-ring-binding TCAT motif, thus perturbing its interaction with GDP.

The loss of local structural stability associated with an increased disorder in the C-terminal part of helix α1 and the N-terminal part of helix α5 is compensated by the strengthening of their interactions with the β4, β5 and β6 strands and the relocated helix α5. This is suggested by the fact that mutation of A220$^{G.S4.1}$ of β4, S263$^{G.S5.1}$ and I265$^{G.S5.3}$of β5, Y320$^{G.S6.2}$ and H322$^{G.S6.4}$ of β6, Q333$^{G.H5.5}$, F334$^{G.H5.6}$, V335$^{G.H5.7}$, and V342$^{G.H5.14}$ of α5 dramatically destabilized the Rho*-G_i complex (20-50%) without affecting the stability of both nucleotide-bound states. Additionally, many of these mutants showed competent heterotrimer reconstitution, while the efficiency in forming the Rho*-G_i complex was reduced by 20-80% (Supplementary Fig. S6). A sequence alignment of human G proteins showed that these residues are highly conserved in the Gα subfamily25. Taken together, this indicates that these residues are not only important for stabilizing the G protein conformation in the receptor-bound state, but also crucial for allosteric regulation of receptor-mediated G protein activation.

Y320 in activation cluster I as a signal transduction hub

Mutation of Y320$^{G.S6.2}$ in the β6 strand, which is a conserved tyrosine or phenylalanine in the Gα subfamily, severely impaired the Rho*-G_i complex formation (Fig. 5a & 6a) while having only a very moderate effect on the nucleotide bound states. Remarkably, Y320A$^{G.S6.2}$, L348A$^{G.H5.20}$, G352A$^{G.H5.24}$ and L353A$^{G.H5.25}$ had a similarly strong impact on the formation of the complex, but Y320$^{G.S6.2}$ is the only position that does not interact

directly with the receptor. Also, Y320A$^{G.S6.2}$ showed a well-preserved ability to bind nucleotides and form the heterotrimer (Supplementary Fig. S6). We hypothesized that mutation of Y320^{CGN} prevented the formation of an allosteric activation pathway that propagates the signal for GDP release transmitted from the receptor, making Y320$^{G.S6.2}$ a key signal transduction hub in the mechanism of receptor-mediated G protein activation.

Cluster II is the structural scaffold of GTPase domain

We identified a second cluster of residues with a common role in the GTPase domain formed by residues in helices α3, α4 and αG packed against residues in strands β4, β5 and β6 (Fig 3 & 5b). While cluster II partially overlapped with cluster I, most mutations here destabilized both receptor- and nucleotide-bound states of $G\alpha_{i1}$. Most mutations destabilized the GDP-bound state by 3-13 ºC, the receptor-bound state by 30-40%, and the GTPγS-bound state by 1-5 ºC (Fig. 5b & 6b). Residues in cluster II are highly conserved among G proteins, and likely form the structural scaffold of the Gα subunit25. It should be noted that mutation of residues I221$^{G.S4.2}$ of β4, T321$^{G.S6.3}$, M247$^{G.H3.6}$ and I253$^{G.H3.12}$, I264$^{G.S5.2}$, N311$^{G.h4s6.2}$ and I319$^{G.S6.1}$ dramatically destabilized R*-Gi complex without affecting the stability of the GDP-bound state (Fig. 6b, Supplementary Table 1). Mutation of K248$^{G.H3.7}$ and D251$^{G.H3.10}$, which are located in solvent-exposed surface, also showed similar effect. We hypothesized that these residues may form additional stabilizing contacts in the receptor-bound conformation, or are involved in direct interactions with the receptor.

Helical domain behaves as a rigid body

A hallmark of G protein activation by the receptor is the release of GDP accompanied by the separation of the GTPase and helical domains. The helical domain consequently displays dynamic equilibrium between multiple orientations relative to the GTPase domain 16,18,19,30. We showed that a cluster of mostly hydrophobic residues (63$^{H.HA.1}$-176$^{H.HF.6}$; stabilization cluster III) of $G\alpha_{i1}$ stabilizes the helical domain (Fig. 3 & 7a, Table. S1). In contrast to the activation and stabilization clusters in the GTPase domain, where most mutants affected both the stability and formation of the Rho*-G_i complex, mutations in the stabilization cluster III did not affect the formation of the Rho*-G_i complex (Fig. 6c & 7a). A sequence alignment shows that hydrophobic residues are preferred at these positions in all Gα subtypes (Supplementary File F1). This is consistent with the observation that the helical domain can be expressed independently from the GTPase domain while retaining its ability to activate cGMP phosphodiesterase 31.

However, there were some exceptions. Mutation of A138$^{H.HD.5}$, L156$^{H.HE.6}$, L159$^{H.HE.9}$, R161$^{H.HE.11}$and I162$^{H.HE.12}$ destabilized the Rho*-G_i complex without affecting the stability of GDP- and GTP-bound states (Fig. 6c, 7a, S6, Supplementary Table 1). Also, I78A$^{H.HA.16}$ reduced complex formation by 20% and L175A$^{H.HF.5}$ destabilized GDP-bound state and reduced complex formation. This suggest that subtle internal rearrangements of the AH domain are required to keep its integrity in the Rho*-G_i complex.

Weakening of the inter-domain interface promotes activation

The inter-domain interface in $G\alpha_{i1}$ is composed by the N-terminal part of helices αA, αF, α1 and loop of αF/α1 (Fig. 3). Mutation of the residues in this interface dramatically destabilized the GDP-bound state (5-14 ºC), but did not destabilize the Rho*-G_i complex. In fact, mutations $K51A^{G.H1.6}$, $K54A^{G.H1.9}$ and $I55A^{G.H1.10}$ increased the relative stability of Rho*-G_i complex by 15-20%. We also observed a similar effect for $L175A^{H.HF.5}$ and $R176A^{H.HF.6}$, which increased complex stability by 9% and 17%, respectively (Fig. 6d, 7b, Table. S1). A sequence alignment showed that the residues located in the inter-domain interface of $G\alpha_{i1}$ are highly conserved in all Gα subfamilies (Supplementary File F1, Flock et al25). Our data suggest that subtle conformational perturbations in the inter-domain interface of GDP-bound state can facilitate the domain separation and the release of GDP, in agreement with previous observations that the helical domain dissociates from the GTPase domain upon binding to the receptor 16–18. The importance of weakening the inter-domain interface for G protein activation is further supported by the structure of the Gα subunit from *Arabidopsis thaliana* (AtGPA1) 32,33. This protein has a structure that is very similar to $G\alpha_{i1}$ (RMSD of 1.8 Å between backbone atoms). However, due to the absence of classical GPCRs in plants, AtGPA1 exchanges nucleotides by a self-activation mechanism attributed to the marginally stable helical domain, which shows a tendency to dissociate from the GTPases domain and unfold. Comparison between the $G\alpha_{i1}$-GDP and AtGPA1 structures shows that they contain similar residues at the inter-domain interface, whereas the cross-interface hydrogen bonds in AtGPA1 are weaker compared to those in $G\alpha_{i1}$-GDP (Supplementary Fig. S7).

Differences between GDP and GTP states

The GTPγS-bound state of $G\alpha_{i1}$ was more stable than the GDP-bound state. The apparent melting temperatures were, respectively, 70 °C and 63 °C at saturating concentrations of the corresponding nucleotides. In addition, GTPγS had a much higher affinity for $G\alpha_{i1}$ compared to GDP, as judged by a steeper concentration dependence of the stabilizing effect (Supplementary Fig. S1). We observed that most mutations destabilized both GDP and GTPγS states, consistent with the relatively minor differences between the GDP- and GTPγS-bound crystallographic structures of $G\alpha_{i1}$. 34. One interesting observation is that the GTPγS bound state was on average two-fold less sensitive to mutations (Supplementary Fig. S8), again suggesting that this is a more stable state. Also, several mutations concentrated around the third phosphate group and at the Gβγ interface had a disproportionally large effect on the GTPγS-bound state. This is precisely the area that undergoes conformational changes associated with the activation of the Gα, causing the dissociation of the α and βγ subunits.

Discussion and Conclusions

The exhaustive coverage (the entire sequence of the $G\alpha_{i1}$ subunit) and single amino acid resolution of our mutagenesis analysis, combined with the stability measurements obtained for $G\alpha_{i1}$ in its GDP-, receptor- and GTPγS-bound states, allowed us to obtain an extremely detailed data set to understand the molecular mechanisms of G protein activation. Our

results showed with that the interactions involved in the stabilization of the receptor-bound conformation of $G\alpha_{i1}$ are broader and more complex that were previously suggested.

First, we identified two clusters of residues that confer stability to the GTPase domain. The activation–cluster I consists of residues in helices α1 and α5 packed against residues in strands β1-3 in the nucleotide-bound states. In the receptor-bound state, the interactions between α5/α1 and β1-3 are weakened and compensated by a new set of interactions between α5 and strands β4-6. The most prominent examples of residues involved in this rearrangement are $Y320^{G.S6.2}$ and $H322^{G.S6.4}$, which are crucial for the stabilization of the receptor-bound state but have no effect on the nucleotide bound state. Conversely, $F336^{G.H5.8}$ is important for the stability of the GDP- and GTP-bound states, but plays little role in the stabilization of the Rho*-G_i complex. Helix α1 is likely to become mostly unstructured in the Rho*-G_i complex, as judged by the absence of significant effect of mutations on complex stability. However, some mutations towards its C-terminal part result in stabilization of the complex. The helix α1 is a recipient of the conformational changes that lead to the destabilization of the inter-domain interface and to nucleotide release, a key step in G protein activation. Mutations in the inter-domain interface between the GTPase and the helical domains, consisting of αA, αF, α1 and loop of αF/α1, dramatically destabilize nucleotide-bound states but do not affect, and some even stabilize, the complex. The above-mentioned residues are just some of the most noticeable examples, but we found a network of residues that contribute to the stabilization of these distinct conformational states (Fig. 3, 5 & 7).

In addition to being able to change its conformation, the G protein also has to maintain its structural integrity and identity during the signaling cycle. Stabilization cluster II includes residues in helices α3, α4 and αG packed against residues in strands β4, β5 and β6. The majority of mutations in this cluster affected similarly both states, and we concluded that this cluster provides a steady structural scaffold to the GTPase domain. As this cluster partially overlaps with the activation cluster I, there were several mutations in strands β4-6, such as $I319^{G.S6.1}$, which preferentially affected the receptor-bound state. A third cluster of residues maintains the structural integrity of the helical domain. Most mutations in this domain resulted in similar effects on the stability of the nucleotide-bound states or the Rho*-G_i complex. Overall, these mutations were less detrimental to the stability than mutations in the GTPase domain. Several mutations, mostly located in helix αH, destabilized the complex without affecting either the GDP- or the GTP-bound state, suggesting that this region undergoes some conformational changes upon receptor binding.

Recently, long-scale molecular dynamics simulations by Dror et al35 suggested that the key events in G protein activation are structural rearrangements in the nucleotide binding site, especially the repositioning of the β6-α5 loop, caused by the movement of helix α5 away from the nucleotide binding site, and a concomitant weakening of the inter-domain interface. They also found that the GDP could only dissociate if the helical domain is in the open conformation. Interestingly, the helical domain remains mostly rigid in the simulations. These findings are very complimentary to our results.

Overall, our data suggest that the most significant event in activation of $G\alpha_{i1}$ is the destabilization of helix α1 caused by a rearrangement on the activation cluster I. This leads to a perturbation and weakening of the inter-domain interface, dissociation of the helical domain from the GTPase domain in a rigid body movement, and release of the GDP (Fig. 8). How does the subsequent binding of GTP trigger dissociation of the complex? The answer may be found in the relative stability of the GDP-, GTP- and receptor bound states. The GTP-bound state of $G\alpha_{i1}$ is thermodynamically the most stable state of the protein, as reflected by the considerably higher thermal stability of the GTPγS-bound state. Due to GTP hydrolysis, the G protein is kinetically trapped in a less stable GDP-bound state. This is a meta-stable state because the nucleotide exchange rate is very low in the absence of the receptor, consistent with proposed role of the helical domain to protect the GDP from exchange with GTP13 readily available in the cytoplasm. As the complex is formed and the nucleotide binding site becomes accessible, the additional stabilization by GTP overcomes the stability of the complex, leads to the stabilization of the helix α1, the inter-domain interface and reverts the helix α5 to its conformation in the nucleotide bound state.

It is still an open question to what extent our findings can be generalized to other GPCR-G protein combinations, and which aspects are specific to the $G\alpha_{i1}$ or the Rho*-G_i complex. However, in Flock et al.25 we show that many of the residues identified here may play similar roles in all G proteins.

Online Materials and Methods

1) Alanine scanning mutagenesis

The alanine scanning expression library of $G\alpha_{i1}$ was prepared as we have reported before 36. The wild-type (WT) plasmid was constructed by inserting human G protein alpha-subunit ($G\alpha_{i1}$) into pJ411 vector (DNA 2.0) which incorporated a N-terminal 10-histidine tag followed by a TEV cleavage site. The alanine mutants were produced based on the WT plasmid by high-throughput (HTP) alanine mutagenesis as we have reported previously 36. All 354 amino acid residues in Gαi1 were mutated. All non-alanine residues were replaced to alanine and alanine residues were substituted to glycine. The exact protein sequence of the construct is provided in the supplementary note.

2) Preparation of native βγ subunit (Gβγ)

Gβγ was separated from endogenous transducin (Gt) as previously described 23. Briefly, dark-adapted bovine retinas (W L Lawson, USA) were exposed to room light at 4 ºC overnight. The rod outer segment (ROS) membranes were collected by centrifugation in a 25-30% (w/w) sucrose gradient. After isotonic and hypotonic washes, Gt was dissociated from ROS membrane by adding GTP (Sigma-Aldrich). The collected Gt was filtered through 0.22 μm membrane (Millipore Corp) and dialyzed against the dialysis buffer (10mM Tris-HCl, pH 7.4, 2 mM $MgCl_2$, 1 mM DTT,) containing 50% glycerol. Gβγ was further separated from the Gαt on a Blue-Sepharose column (GE Healthcare) by a linear salt gradient (0-500 mM NaCl) in the dialysis buffer supplemented with 30% glycerol. The Gβγ was concentrated to 1-5 mg/ml and stored at -80 °C.

3) Preparation of bovine rhodopsin

Bovine rhodopsin was extracted from dark-adapted ROS membranes which were prepared according to Okada's method 37. The dark-adapted ROS membranes were solubilized in solubilization buffer (50 mM sodium acetate, pH 6, 1 mM EDTA, 2 mM 2-mercaptoethanol, 3 mM $CaCl_2$, 3 mM $MgCl_2$, 3 mM $MnCl_2$, 100 mM NaCl) supplemented with 80 mM (4.1%) β-dodecyl-D-n-maltoside (DDM) at 4 ºC overnight. After centrifugation at 30,000 rpm in a Ti70 rotor, the supernatant was diluted with solubilization buffer to a concentration of DDM as 0.4%. The diluted sample was loaded to a column packed with ConA Sepharose resin (GE Healthcare) which was equilibrated with washing buffer (solubilization buffer supplemented with 0.02% DDM). After extensive washing, bovine rhodopsin was eluted with solubilization buffer supplemented with 0.02% DDM and 0.2 M α-D-methylmannoside. The eluted bovine rhodopsin was concentrated to 1-4 mg/ml and stored at -80 °C.

4) High throughput (HTP) culturing and purification of $G\alpha_{i1}$ alanine mutants

The recombinant Gαi1 alanine mutants were expressed in BL21 (DE3) competent cells. The cultures were grown at 37 ºC in TB media (GERBU Biotechnik GmbH) by using 24 well plates (mutant/well) (Whatman UniFilter Microplates, GE Healthcare). The culture volume was 5 ml/well. When the OD600 reached 0.6, cells were induced with 0.5 mM IPTG and continued to grow for 20 hours at 20 ºC. The cell were harvested by centrifugation resuspended in the binding buffer (25 mM Tris-HCl, pH 7.4, 500 mM NaCl, 10% glycerol, 50 mM imidazole, 5 mM 2-mercaptoethanol) and transferred to a 96 deep-well plate (Thermo Scientific). The re-suspended cells were disrupted by sonication for 1 min using a SONICS VCX-600 sonicator equipped with an 8-pin probe. After clarifying cell lysates by centrifugation, the supernatants were loaded to a 96 deep-well filter plate (one mutant per well) pre-loaded with 500 µl cobalt chelating resin (GE Healthcare) and equilibrated with binding buffer. After extensive washing with binding buffer, the recombinant Gαi1 alanine mutants were eluted with elution buffer (25 mM Tris-HCl, pH 7.4, 500 mM NaCl, 10% glycerol, 500 mM imidazole, 5 mM 2-mercaptoethanol). The eluted proteins were dialyzed against 25 mM Hepes, pH 7.4, 100 mM NaCl and 2 mM DTT using Slide-A-Lyzer MINI Dialysis Device (Thermo Scientific). Among of 354 alanine mutants, the purified $R142A^{H.HD.9}$, $Y230A^{G.s4h3.4}$, $K270A^{G.s5hg.1}$ and $D272A^{G.HG.2}$ were severely aggregated and could not be used in the further assays. The flowchart of HTP purification is shown in Supplementary Fig. S1.

5) Characterization of the effect of $G\alpha_{i1}$ alanine mutants on the receptor-bound state by a HTP assay

In each round, WT $G\alpha_{i1}$ was always prepared in parallel with the $G\alpha_{i1}$ alanine mutants [$G\alpha_{i1}$(Ala)] to form rhodopsin-G_i protein complex [Rho*-G_i(WT)] as the reference control. The recombinant $G\alpha_{i1}$ alanine mutants (12.5 µM) from HTP purification and the native $G\beta\gamma_t$ (10 µM) were reconstituted to form heterotrimer (G_i) by incubation in a 96-well PCR plate (one mutant per well) (Eppendorf) on ice for 2 h. Under the dim-red light in the dark room, purified rhodopsin (18 µM) was added and mixed with G_i in ice-cold assay buffer (25 mM Hepes, pH 7.4, 100 mM NaCl, 2mM DTT, 0.02% DDM, 1 mM $MgCl_2$, 0.16 unit/ml

apyrase). After irradiation with orange light (>495 nm) on ice for 10 min, the tetramer complex Rho*-G_i(Ala) was formed by coupling the activated rhodopsin with G_i and the formed Rho*-G_i(Ala) complex was further incubated in the dark at 4 ºC overnight. The reaction volume was 50 μl for each alanine mutant. 20 μl of each Rho*-G_i(Ala) complex was transferred to another 96-well PCR plate and heated for 30 min in a PCR machine (Eppendorf Mastercycler Gradient) at 36.3 ºC. After centrifugation at 3000 rpm for 10 min at 4 ºC, 14 μl of formed Rho*-G_i(Ala) complex (4 ºC) and 14 μl of heated Rho*-G_i(Ala) complex (36.3 ºC) were mixed with NativePAGE Sample Buffer (4×) (Invitrogen) and NativePAGE 5% G-250 Sample Additive (Invitrogen), respectively. The mixtures were loaded onto 4-16% NativePAGE Bis-Tris-HCl Gels (Invitrogen) and gel electrophoresis was performed in a 4 ºC cold room according to the manufacturer's protocol (Invitrogen). Protein markers were used with NativeMark Unstained Protein Standard (Invitrogen). The gel bands of Rho*-G_i complex were integrated and quantified using the ImageJ software. The complex formation efficiency (CF) (%) was obtained from the normalization of integrated density of Rho*-G_i complex band [ID_C(Ala or WT), 4 ºC] with integrated density of Rho*-G_i(WT) complex band [IDC(WT), 4 ºC]. The complex stability (CS) (%) was defined as the normalization of integrated density of Rho*-G_i complex band [ID_C(Ala or WT), 36.3 ºC] with integrated density of Rho*-G_i(WT) complex band [ID_C(Ala or WT), 4 ºC].

$$\mathrm{CF(Ala)}=\frac{\mathrm{ID_C(Ala,\ 4^\circ C)}}{\mathrm{ID_C(WT,\ 4^\circ C)}}\times 100\%$$
$$\mathrm{CS(WT)}=\frac{\mathrm{ID_C(WT,\ 36.3^\circ C)}}{\mathrm{ID_C(WT,\ 4^\circ C)}}\times 100\%$$
$$\mathrm{CS(Ala)}=\frac{\mathrm{ID_C(Ala,\ 36.3^\circ C)}}{\mathrm{ID_C(Ala,\ 4^\circ C)}}\times 100\%$$

The ΔCF (%) and ΔCS (%) were defined as:

$$\Delta\mathrm{CF}=\mathrm{CF(Ala)}-\mathrm{CF(WT)}$$
$$\Delta\mathrm{CS}=\mathrm{CS(Ala)}-\mathrm{CS(WT)}$$

The distribution and summary of ΔCF efficiency and ΔCS of each Gαi1 alanine mutant are listed in Fig. 2 and Supplementary Table 1. The flowchart diagram of HTP assay is shown in Supplementary Fig. S2.

6) HTP measurements of thermal stability Gαi1 alanine mutants by differential scanning fluorimetry (DSF)

The thermostability of each $G\alpha_{i1}$ alanine mutant in the nucleotide-bound states was measured by HTP differential scanning fluorimetry (DSF). The samples were prepared on ice. 10 μl of recombinant $G\alpha_{i1}$ alanine mutant stocks (0.7 μg/μl) were dispensed into a 96-well PCR plate (one mutant per well) (Eppendorf) and mixed with 100 μl ice-cold assay buffer (25mM Hepes, pH 7.4, 100mM NaCl, 2mM DTT) containing 5× SYPRO-orange (Invitrogen) and nucleotides (1 mM GDP or 100 μM GTPγS). After mixing, 110 μl reaction mixture of each alanine mutant was divided into 0.2 ml PCR tubes (Qiagen) as three samples of 35 μl. The DSF experiments were performed with Rotor GeneQ (Qiagen) by ramping from 25 °C to 95 °C at a rate of 3 °C/min. The melting temperature (T_m) was defined as the

inflection point of the melting curve as analyzed by the Rotor Gene Q Series Software. The T_m value of each $G\alpha_{i1}$ alanine mutant [T_m(Ala)] upon addition of the nucleotides was averaged from three individual experiments.

The ΔT_m value was defined as:

$$\Delta T_m = T_m(\text{Ala}) - T_m(\text{WT})$$

In each round, WT $G\alpha_{i1}$ was always prepared in parallel with $G\alpha_{i1}$ alanine mutants as a reference control.

In addition, the thermal shift of WT $G\alpha_{i1}$ in titration with GDP and GTPγS were also performed with HTP DSF.

7) Analysis of heterotrimer formation by fluorescence assisted size exclusion chromatography (FSEC)

The recombinant $G\alpha_{i1}$ alanine mutants (6 μM) and $G\beta\gamma_t$ (2 μM) were reconstituted to form heterotrimer (G_i) in 100 μl running buffer (25 mM Hepes, pH 7.4, 100 mM NaCl) overnight on ice. 80 μl of reconstituted G_i was injected to Superdex 200 packed in a Tricorn 10/200 column (GE Healthcare) equilibrated with the running buffer. The elution profile was monitored by protein-intrinsic fluorescence with λex: 280 nm and λem: 340 nm at a flow rate of 1 ml/min. The retention time of the reconstituted G_i was integrated with UNICORN 5.2 software (GE Healthcare).

8) Modelling of the rhodopsin/Gi complex

Homology modelling of $G\alpha_{i1}$—The sequences of $G\alpha_{i1}$ and $G\alpha_s$ were aligned using Clustal Omega 38. This initial alignment was manually refined using Chimera 39 to adjust some of the gaps in the loop regions. Using this alignment, $G\alpha_{i1}$ was modelled with Modeller 40 using the structure of Gs bound to the beta 2 adrenergic receptor 16 as a template. Residues missing in the template were refined using the loop optimization method in Modeller. All models were subjected to 300 iterations of variable target function method optimization and thorough molecular dynamics and simulated annealing optimization and scored using the discrete optimized protein energy potential. The 20 best-scoring models were analyzed visually, and a suitable model (in terms of low score and structure of the loops) was selected.

Homology modelling of active rhodopsin—The sequences of bovine rhodopsin and the human beta 2 adrenergic receptor were aligned using Clustal Omega 38. This initial alignment was manually refined using Chimera 39 to adjust some of the gaps in the loop regions. Using this alignment, rhodopsin was modelled with Modeller 40 using the structure of the beta 2 adrenergic receptor bound to Gs 16 as a template. Residues missing in the template were refined using the loop optimization method in Modeller. All models were subjected to 300 iterations of variable target function method optimization and thorough molecular dynamics and simulated annealing optimization and scored using the discrete

optimized protein energy potential. The 20 best-scoring models were analyzed visually, and a suitable model (in terms of low score and structure of the loops) was selected.

Modelling of the rhodopsin - Gi complex—The models of $G\alpha_{i1}$ and rhodopsin were superimposed to the structures of $G\alpha_s$ and the beta 2 adrenergic receptor 16, keeping the G beta and gamma subunits. In addition to the crystallographic waters resolved in the structure of rhodopsin, we added additional ordered water molecules, as observed in the high-resolution structure of the adenosine A2A receptor 41. Cysteines 322 and 323 were palmitoylated. Glu, Asp, Arg and Lys residues were set as charged, except Glu122(3.37) and Asp83(2.50) 42. Topology and parameter definitions for palmitoyl-cysteine and retinal bound via protonated Schiff-base link to lysine 43,44 were obtained from the parameter/topology repository of NAMD 45. The complex was embedded in a solvated and pre-equilibrated lipid bilayer consisting of 360 molecules of 1-palmitoyl-2-oleoyl-sn-glycerol-3-phosphatidylcholine (POPC) and approx. 50.000 water molecules. Sodium and chloride ions were added to a concentration of 0.15M NaCl, and then additional ions were added to achieve charge neutrality. The system measured roughly 120 × 120 × 160 Å^3, with a total of approximately 215'000 atoms. This system was equilibrated as follows: first a short (0.5 ns) simulation was performed in which only the lipid tails were allowed to move, in order to induce the appropriate disorder of a fluid-like bilayer. Then, the geometry of the entire system was optimized by 1000 steps of energy minimization, followed by two equilibration steps with the protein constrained (0.5 ns) and without constraints (0.5 ns). In order to equilibrate the complex, the system was subjected to 20 ns of unrestrained molecular dynamics. Simulations were carried out using NAMD 2.8 45 with the CHARMM27 all-hydrogen force field 46 at constant pressure (1 atm), and using a time step of 2 fs.

Supplementary Material

Refer to Web version on PubMed Central for supplementary material.

Acknowledgements

We thank F. Heydenreich, V. Korkhov, R. Kammerer and C. Piscitelli for the critical reading of the manuscript, and V. Panneels and R. Jaussi for technical support. S. Maeda was supported by the Roche postdoctoral fellowship RPF113. T.F. is Boehringer Ingelheim Fonds PhD fellow. D. M. and S. Mendieta were supported by the Paul Scherrer Institute internship program. This work was supported by Swiss National Science Foundation grants Sinergia 141898 (D.B.V., G.F.X.S.), 133810 31-135754 (D.B.V.), 31-153145 (G.F.X.S.), 31003A-146520 (X.D.), National Centre of Competence in Research (NCCR) Structural Biology, NCCR Molecular Systems Engineering, European Cooperation in Science and Technology Action CM1207 GLISTEN: GPCR-Ligand Interactions, Structures, and Transmembrane Signalling: a European Research Network (X.D. and G.F.X.S.), the Marie Curie Initial Training Network NanoMem (D.B.V., G.F.X.S.), the Medical Research Council (MC_U105185859; M.M.B., T.F.) and the. M.M.B. is a Lister Institute Research Prize Fellow. Molecular dynamics simulations were run at the Swiss National Supercomputing Centre (CSCS).

References

1. Gilman AG. G proteins: transducers of receptor-generated signals. Annu Rev Biochem. 1987; 56:615–49. [PubMed: 3113327]
2. Wall MA, et al. The structure of the G protein heterotrimer Gi alpha 1 beta 1 gamma 2. Cell. 1995; 83:1047–58. [PubMed: 8521505]
3. Sprang SR. G proteins, effectors and GAPs: structure and mechanism. Curr Opin Struct Biol. 1997; 7:849–56. [PubMed: 9434906]

4. Oldham WM, Van Eps N, Preininger AM, Hubbell WL, Hamm HE. Mechanism of the receptor-catalyzed activation of heterotrimeric G proteins. Nature structural & molecular biology. 2006; 13:772–7.
5. Oldham WM, Hamm HE. Heterotrimeric G protein activation by G-protein-coupled receptors. Nat Rev Mol Cell Biol. 2007
6. Marin EP, Krishna AG, Sakmar TP. Rapid activation of transducin by mutations distant from the nucleotide-binding site: evidence for a mechanistic model of receptor-catalyzed nucleotide exchange by G proteins. The Journal of biological chemistry. 2001; 276:27400–5. [PubMed: 11356823]
7. Marin EP, Krishna AG, Sakmar TP. Disruption of the alpha5 helix of transducin impairs rhodopsin-catalyzed nucleotide exchange. Biochemistry. 2002; 41:6988–94. [PubMed: 12033931]
8. Garcia PD, Onrust R, Bell SM, Sakmar TP, Bourne HR. Transducin-alpha C-terminal mutations prevent activation by rhodopsin: a new assay using recombinant proteins expressed in cultured cells. The EMBO journal. 1995; 14:4460–9. [PubMed: 7556089]
9. Onrust R, et al. Receptor and betagamma binding sites in the alpha subunit of the retinal G protein transducin. Science. 1997; 275:381–4. [PubMed: 8994033]
10. Coleman DE, et al. Structures of active conformations of Gi alpha 1 and the mechanism of GTP hydrolysis. Science. 1994; 265:1405–12. [PubMed: 8073283]
11. Mixon MB, et al. Tertiary and quaternary structural changes in Gi alpha 1 induced by GTP hydrolysis. Science. 1995; 270:954–60. [PubMed: 7481799]
12. Chen Z, Singer WD, Danesh SM, Sternweis PC, Sprang SR. Recognition of the activated states of Galpha13 by the rgRGS domain of PDZRhoGEF. Structure. 2008; 16:1532–43. [PubMed: 18940608]
13. Noel JP, Hamm HE, Sigler PB. The 2.2 A crystal structure of transducin-alpha complexed with GTP gamma S. Nature. 1993; 366:654–63. [PubMed: 8259210]
14. Lambright DG, Noel JP, Hamm HE, Sigler PB. Structural determinants for activation of the alpha-subunit of a heterotrimeric G protein. Nature. 1994; 369:621–8. [PubMed: 8208289]
15. Lambright DG, et al. The 2.0 A crystal structure of a heterotrimeric G protein. Nature. 1996; 379:311–9. [PubMed: 8552184]
16. Rasmussen SG, et al. Crystal structure of the beta2 adrenergic receptor-Gs protein complex. Nature. 2011; 477:549–55. [PubMed: 21772288]
17. Van Eps N, et al. Interaction of a G protein with an activated receptor opens the interdomain interface in the alpha subunit. Proc Natl Acad Sci U S A. 2011
18. Westfield GH, et al. Structural flexibility of the G alpha s alpha-helical domain in the beta2-adrenoceptor Gs complex. Proc Natl Acad Sci U S A. 2011; 108:16086–91. [PubMed: 21914848]
19. Gales C, et al. Probing the activation-promoted structural rearrangements in preassembled receptor-G protein complexes. Nature structural & molecular biology. 2006; 13:778–86.
20. Chung KY, et al. Conformational changes in the G protein Gs induced by the beta2 adrenergic receptor. Nature. 2011; 477:611–5. [PubMed: 21956331]
21. Alexander NS, et al. Energetic analysis of the rhodopsin-G-protein complex links the alpha5 helix to GDP release. Nature structural & molecular biology. 2014; 21:56–63.
22. Kaya AI, et al. A conserved phenylalanine as a relay between the alpha5 helix and the GDP binding region of heterotrimeric Gi protein alpha subunit. The Journal of biological chemistry. 2014; 289:24475–87. [PubMed: 25037222]
23. Maeda S, et al. Crystallization scale preparation of a stable GPCR signaling complex between constitutively active rhodopsin and G-protein. PLoS ONE. 2014; 9:e98714. [PubMed: 24979345]
24. Matouschek A, Kellis JT Jr, Serrano L, Fersht AR. Mapping the transition state and pathway of protein folding by protein engineering. Nature. 1989; 340:122–6. [PubMed: 2739734]
25. Flock T, et al. Universal allosteric mechanism for Galpha activation by GPCRs. Nature. 2015
26. Hamm HE, et al. Site of G protein binding to rhodopsin mapped with synthetic peptides from the alpha subunit. Science. 1988; 241:832–5. [PubMed: 3136547]
27. Osawa S, Weiss ER. The effect of carboxyl-terminal mutagenesis of Gt alpha on rhodopsin and guanine nucleotide binding. J Biol Chem. 1995; 270:31052–8. [PubMed: 8537363]

28. Standfuss J, et al. The structural basis of agonist-induced activation in constitutively active rhodopsin. Nature. 2011; 471:656–60. [PubMed: 21389983]
29. Dratz EA, et al. NMR structure of a receptor-bound G-protein peptide. Nature. 1993; 363:276–81. [PubMed: 8487866]
30. Van Eps N, et al. Interaction of a G protein with an activated receptor opens the interdomain interface in the alpha subunit. Proc Natl Acad Sci U S A. 2011; 108:9420–4. [PubMed: 21606326]
31. Liu W, Northup JK. The helical domain of a G protein alpha subunit is a regulator of its effector. Proceedings of the National Academy of Sciences of the United States of America. 1998; 95:12878–83. [PubMed: 9789008]
32. Jones JC, et al. The crystal structure of a self-activating G protein alpha subunit reveals its distinct mechanism of signal initiation. Sci Signal. 2011; 4:ra8. [PubMed: 21304159]
33. Urano D, Chen JG, Botella JR, Jones AM. Heterotrimeric G protein signalling in the plant kingdom. Open Biol. 2013; 3:120186. [PubMed: 23536550]
34. Raw AS, Coleman DE, Gilman AG, Sprang SR. Structural and biochemical characterization of the GTPgammaS-, GDP.Pi-, and GDP-bound forms of a GTPase-deficient Gly42 --> Val mutant of Gialpha1. Biochemistry. 1997; 36:15660–9. [PubMed: 9398294]
35. Dror RO, et al. SIGNAL TRANSDUCTION. Structural basis for nucleotide exchange in heterotrimeric G proteins. Science. 2015; 348:1361–5. [PubMed: 26089515]
36. Sun D, et al. AAscan, PCRdesign and MutantChecker: a suite of programs for primer design and sequence analysis for high-throughput scanning mutagenesis. PLoS ONE. 2013; 8:e78878. [PubMed: 24205336]
37. Iwata, S. Methods and results in crystallization of membrane proteins. International University Line; La Jolla, CA: 2003.
38. Sievers F, et al. Fast, scalable generation of high-quality protein multiple sequence alignments using Clustal Omega. Mol Syst Biol. 2011; 7:539. [PubMed: 21988835]
39. Pettersen EF, et al. UCSF Chimera--a visualization system for exploratory research and analysis. J Comput Chem. 2004; 25:1605–12. [PubMed: 15264254]
40. Webb, B.; Sali, A. Comparative Protein Structure Modeling Using MODELLER. Current Protocols in Bioinformatics. John Wiley & Sons, Inc.; 2002.
41. Liu W, et al. Structural basis for allosteric regulation of GPCRs by sodium ions. Science. 2012; 337:232–6. [PubMed: 22798613]
42. Mahalingam M, Martinez-Mayorga K, Brown MF, Vogel R. Two protonation switches control rhodopsin activation in membranes. Proc Natl Acad Sci U S A. 2008; 105:17795–800. [PubMed: 18997017]
43. Tajkhorshid E, Baudry J, Schulten K, Suhai S. Molecular dynamics study of the nature and origin of retinal's twisted structure in bacteriorhodopsin. Biophys J. 2000; 78:683–93. [PubMed: 10653781]
44. Nina M, Roux B, Smith JC. Functional interactions in bacteriorhodopsin: a theoretical analysis of retinal hydrogen bonding with water. Biophys J. 1995; 68:25–39. [PubMed: 7711248]
45. Phillips JC, et al. Scalable molecular dynamics with NAMD. J Comput Chem. 2005; 26:1781–802. [PubMed: 16222654]
46. MacKerell AD, et al. All-atom empirical potential for molecular modeling and dynamics studies of proteins. J Phys Chem B. 1998; 102:3586–616. [PubMed: 24889800]

Europe PMC Funders Author Manuscripts

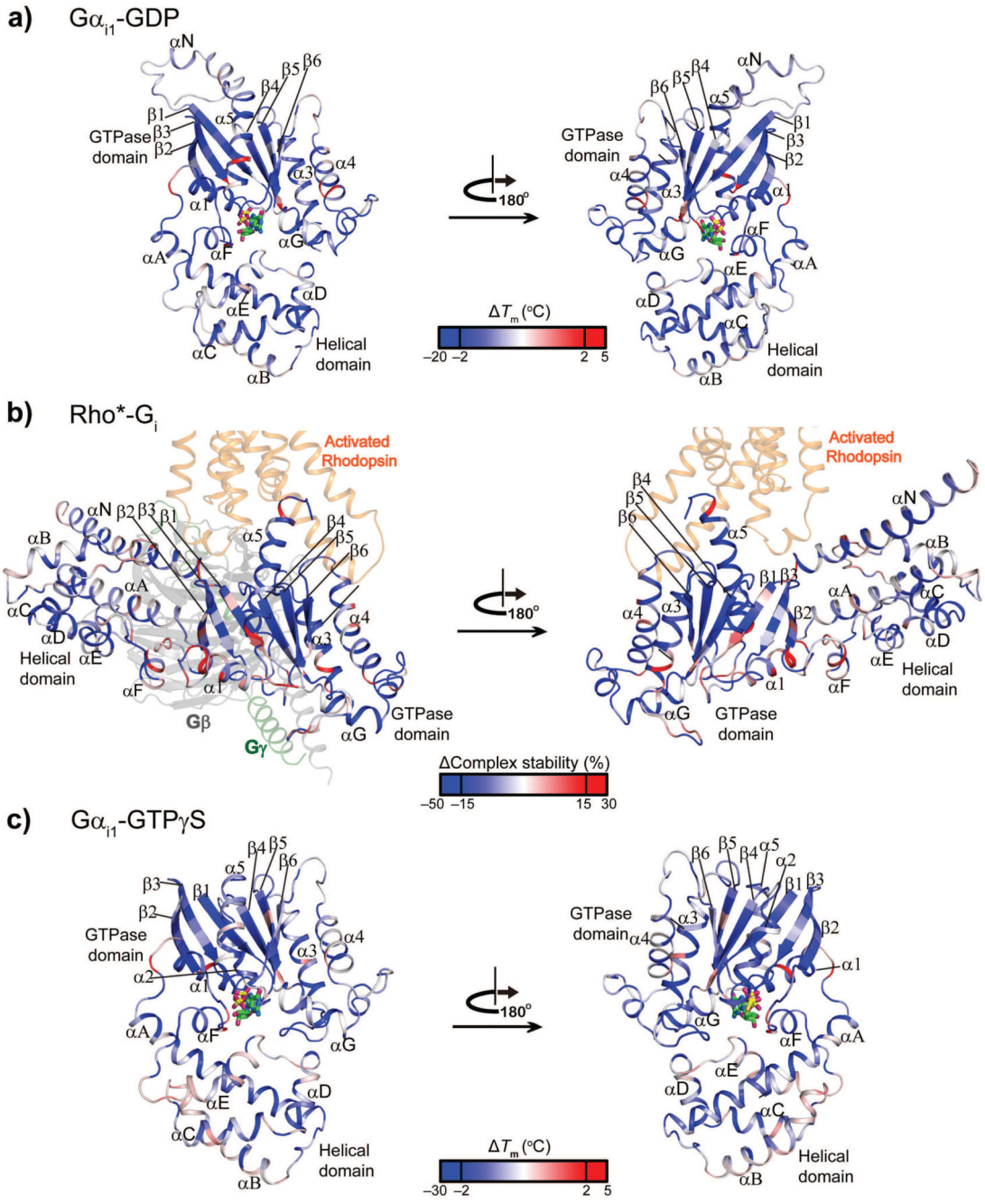

Figure 1. Stability effects of Gα$_{i1}$ alanine mutants on the nucleotide-bound and receptor-bound states.

a-c, Effects of alanine substitutions in Gα$_{i1}$ on stability of the (a) GDP-, (b) receptor- and (c) GTPγS–bound states. In the GDP- **(a)**and GTPγS-bound **(b)** states, the ΔT_m values for each single alanine mutant are mapped onto the crystal structure of GDP-bound Gα$_{i1}$ (PDB 1GDD11) and GTPγS-bound Gα$_{i1}$ (PDB 1GIA10), as a spectrum ranging from blue over white to red. In the receptor-bound state **(b)**, the change in the complex stability (Δcomplex stability) is mapped onto the homology model of Rho*-G$_i$ complex (see supplementary

Europe PMC Funders Author Manuscripts

methods) as spectrum ranging from blue over white to red. Rhodopsin is shown in orange. β and γ subunits are displayed in grey and forest green, respectively. GDP and GTPγS are shown as sticks. The view of GTPase domain of $G\alpha_{i1}$ in the complex-bound state is the same as in the GDP- and GTP-bound state, while the helical domain is significantly displaced relative to the GTPase domain in the receptor-bound state.

Europe PMC Funders Author Manuscripts

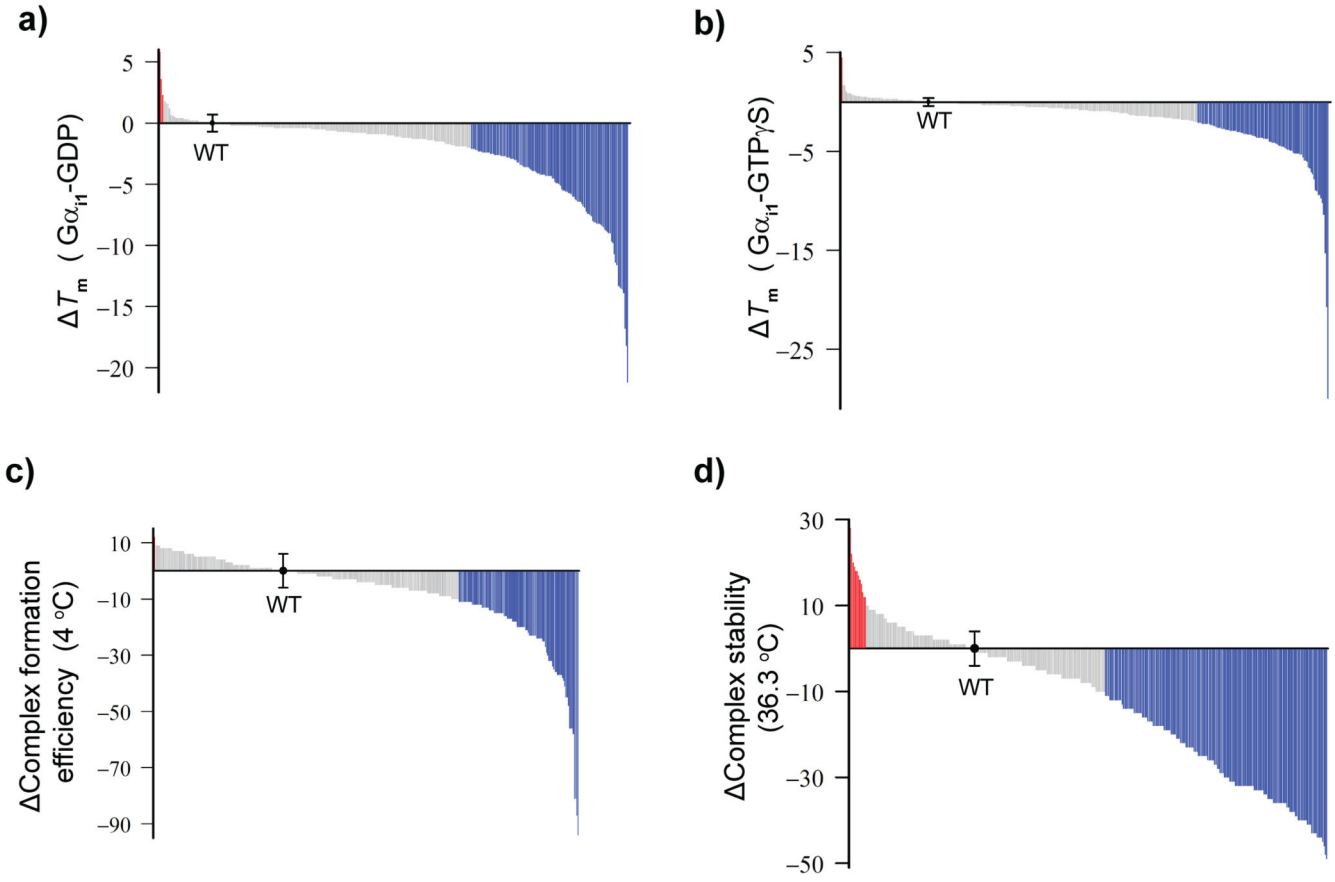

Figure 2. Distribution of effects of Gα$_{i1}$ alanine mutants on the nucleotide-bound and receptor-bound states.

a, **b**, Changes in stability (ΔT_m) of Gα$_{i1}$(Ala)-GDP (w/ 1mM GDP) (**a**) and ΔT_m of Gα$_{i1}$(Ala)-GTPγS (w/ 0.1mM GTPγS) (**b**). Gray: -2°C < ΔT_m < 2°C; blue: ΔT_m < -2°C; red: 2°C < ΔT_m. The ΔT_m of Gα$_{i1}$(WT)-GDP or -GTPγS was shown as the black dot. **c**, Distribution of Δ complex formation efficiency of Rho*-G$_i$(Ala). Blue: Δ complex formation efficiency is less than -10%; gray: between -10% and 10%; red: more than 10%. **d**, Distribution of Δcomplex stability of Rho*-G$_i$(Ala). Blue: Δcomplex stability is less than -10%; gray: between -10% and 10%; red: more than 10%. The definition of ΔT_m, Δcomplex formation efficiency, and Δcomplex stability are described in the methods section. All data are presented in Supplementary Table 1. As for ΔT_m of Gα$_{i1}$ (WT)-GDP and Gα$_{i1}$(Ala)-GTPγS, data points represent mean ± s.d. from 25 and 24 individual experiments, respectively. As for Δcomplex formation efficiency and Δcomplex stability of Rho*-G$_i$(WT), data points represent mean ± s.d. of 33 and 38 individual experiments, respectively.

Europe PMC Funders Author Manuscripts

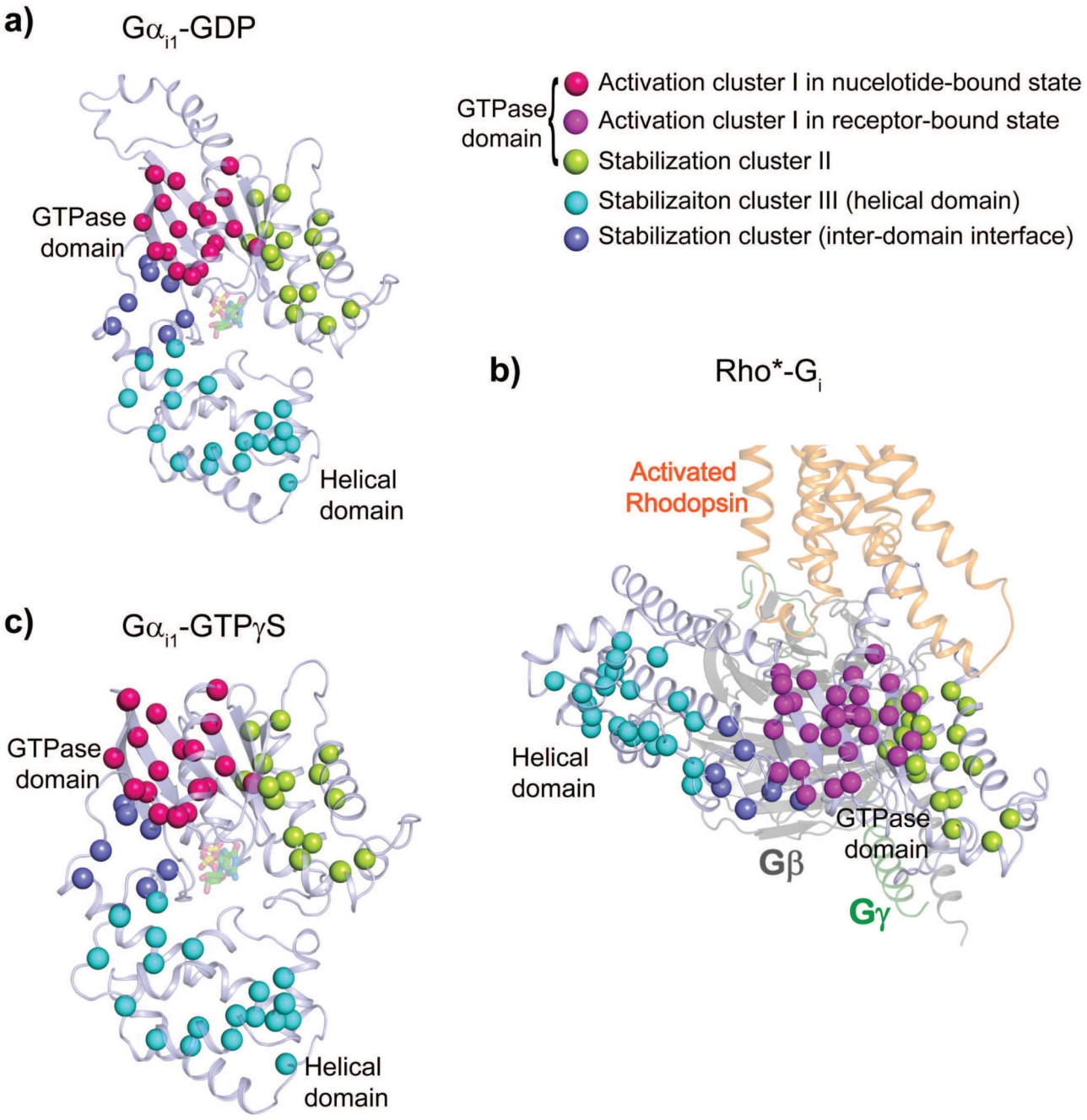

Figure 3. Stabilization clusters in the GTPase, helical domain and the inter-domain interface in the nucleotide- and receptor-bound states.

a-c, Identified stabilization clusters derived from stability effects of $G\alpha_{i1}$ alanine mutants on GDP- (**a**), receptor- (**b**) and GTP γS-bound (**c**) states. The identified activation cluster I and stabilization cluster II in the GTPase domain, the stabilization cluster III in the helical domain, and the stabilization cluster in the inter-domain interface are shown as spheres and mapped to GDP-bound $G\alpha_{i1}$ state (PDB 1GDD 11) (**a**), homology model of Rho*-G_i complex state (**b**) and GTP γS-bound $G\alpha_{i1}$ state (PDB 1GIA 10) (**c**). The stabilization

cluster II, III and the stabilization cluster in the inter-domain interface are coloured in lemon, cyan and slate blue spheres in all three states, respectively. The activation cluster I is displayed as hot pink spheres in nucleotide-bound state (**a**, **c**), and as magenta spheres in the receptor-bound state (**b**) to indicate its conformational change upon coupling to the receptor. The relative orientation of the GTPase domain is identical in all states, while the helical domain is displaced in the receptor-bound state.

Europe PMC Funders Author Manuscripts

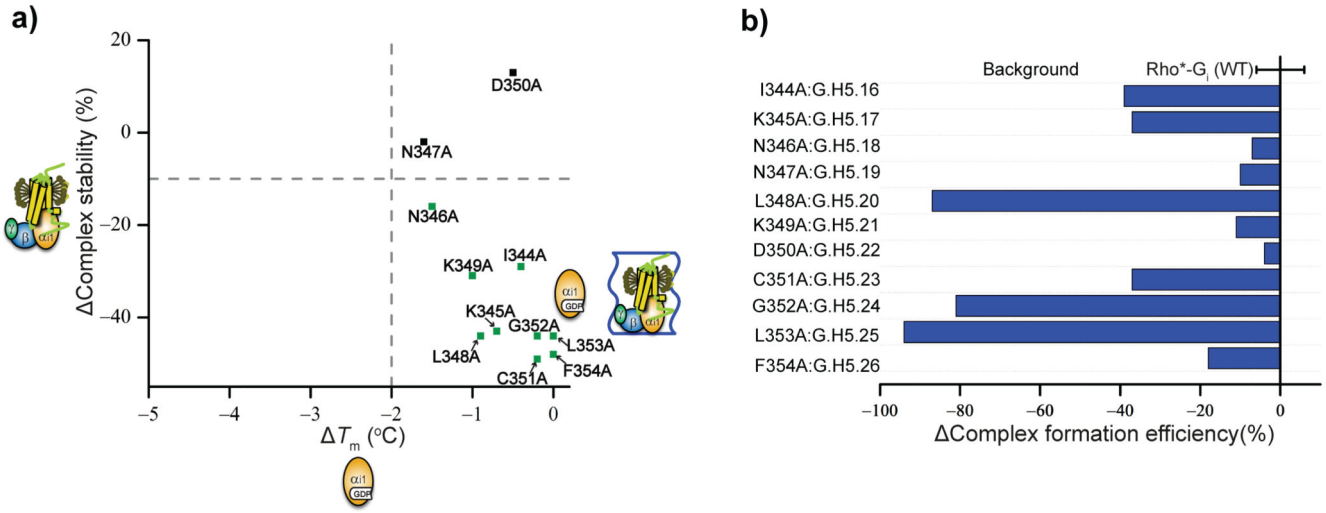

Figure 4. Effect on the nucleotide-bound and receptor-bound states of alanine mutation of the last 11 amino acids of $G\alpha_{i1}$.

a, Effect on the thermal stability of the GDP-bound and receptor-bound states of alanine mutation of the last 11 resides of the C-terminus of $G\alpha_{i1}$. The CGN of the labelled residues is listed in Supplementary Table 1. **b**, Effect on Rho*-G_i complex formation of alanine mutation of the last 11 resides of the C-terminus of $G\alpha_{i1}$. The increase in Δcomplex formation efficiency is coloured in red and the decrease is coloured in blue. The definition of ΔT_m, Δ complex formation efficiency, and Δcomplex stability are provided in the supplementary methods and the derived numbers are shown in Supplementary Table 1. Data points represent mean ± s.d. of 33 individual experiments.

Europe PMC Funders Author Manuscripts

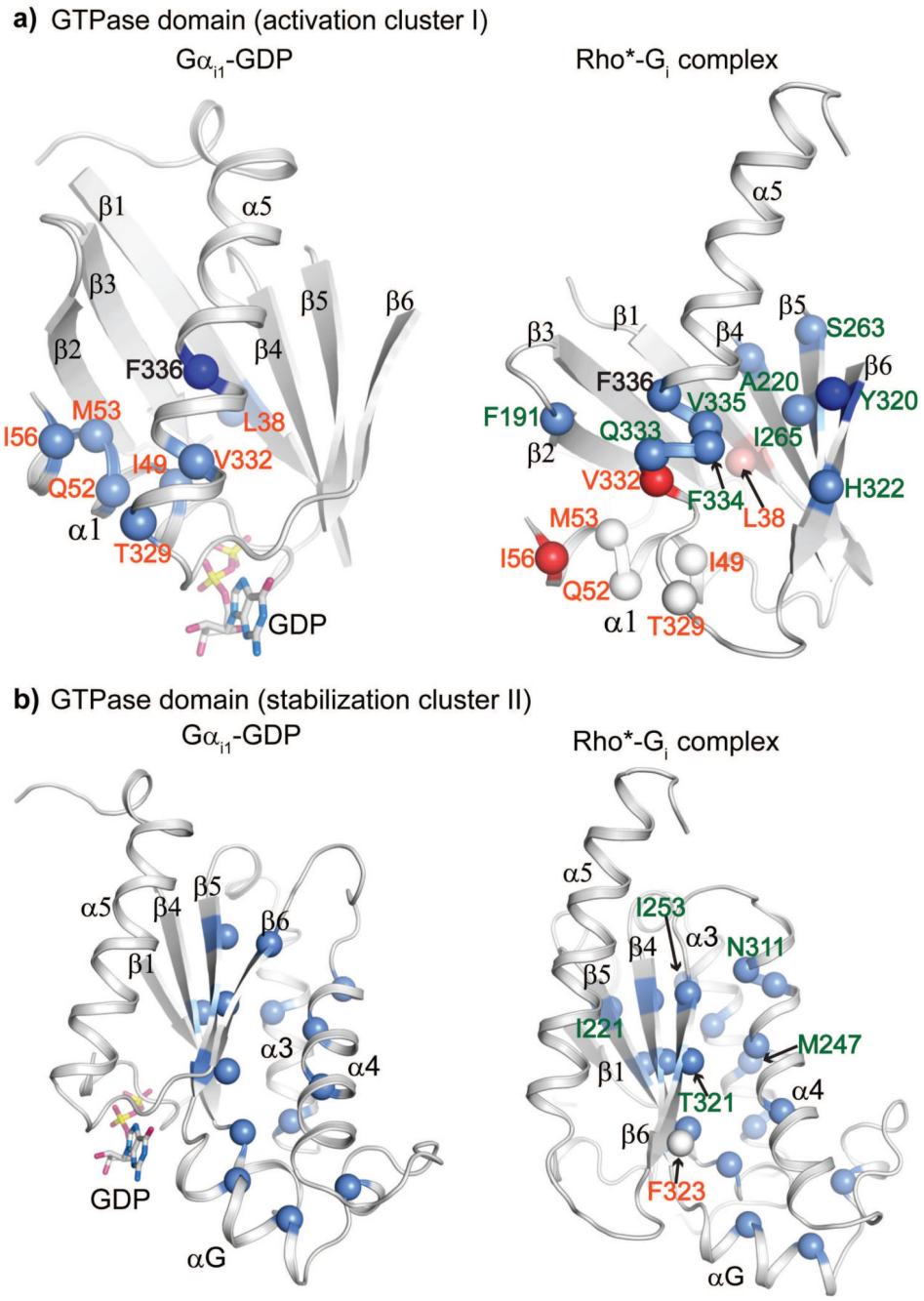

Figure 5. Close-up view of activation cluster I and stabilization cluster II.

a-b, Residues involved in the activation cluster I (**a**) and the stabilization cluster II (**b**) of the GTPase domain in GDP-bound and receptor-bound states. The involved residues are shown as spheres in both the GDP-bound and receptor-bound states. Light blue: destabilizing effect by mutation to alanine; white: stability comparable to WT after mutation to alanine; light red: stabilizing effect due to mutation to alanine. Residues labelled in orange: alanine mutations dramatically destabilize the GDP-bound state but not the receptor-bound state; residues labelled in forest green: alanine mutations do not affect the GDP-bound state, but

significantly destabilize the receptor-bound state; residues without labeling: alanine mutation destablizie both GDP- and receptor-bound state. I56A$^{G.H1.11}$ and V332A$^{G.H5.4}$ (shown in red) significantly stabilize the complex. The alanine mutation of F336$^{G.H5.8}$ completely impairs the stability of the GDP-bound state (shown in deep blue). The alanine mutation of Y320$^{G.S6.2}$ severely impairs the complex formation (shown in deep blue). The CGN of the labelled residues is listed in Supplementary Table 1.

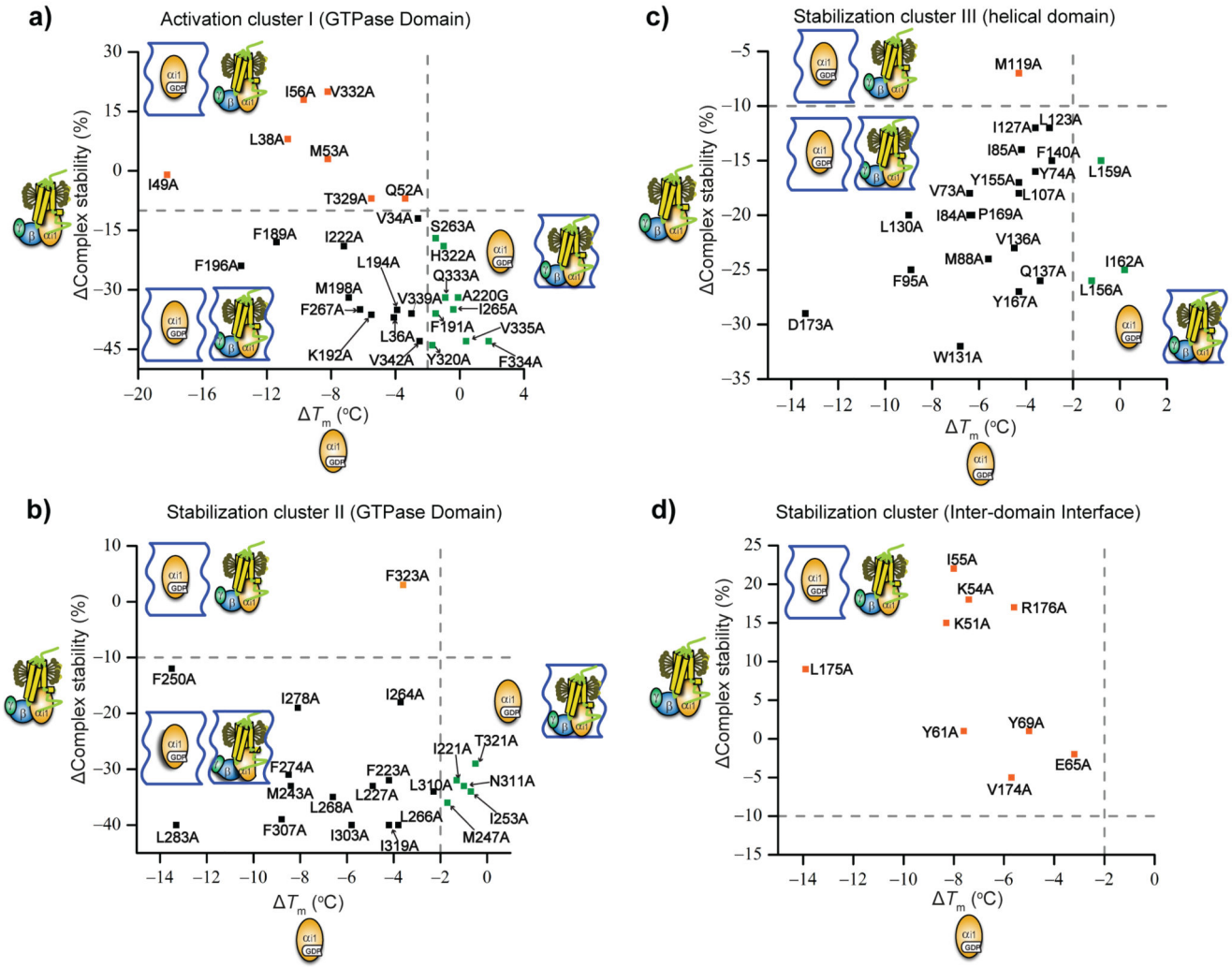

Figure 6. Stability effect of alanine mutation of the residues involved in the activation and stabilization clusters.

a-d, Effect on stability of mutation of the residues involved in the activation cluster I (**a**), stabilization clusters II (**b**) and III (**c**), and the inter-domain interface (**d**) on the GDP- and receptor-bound states. Orange: mutations that dramatically destabilize the GDP-bound state, but do not affect the stability of receptor-bound state; forest green: mutations that do not destabilize the GDP-bound state, but significantly destabilize the receptor-bound state; black: mutation that destabilize both nucleotide- and receptor-bound states. The alanine mutants represented by the orange and the forest green box correspond to the colour of residue number shown in Fig. 5a-b and Fig. 7a-b. The blue wavy box cartoons represent the nucleotide- or receptor-bound states affected by mutations.

Europe PMC Funders Author Manuscripts

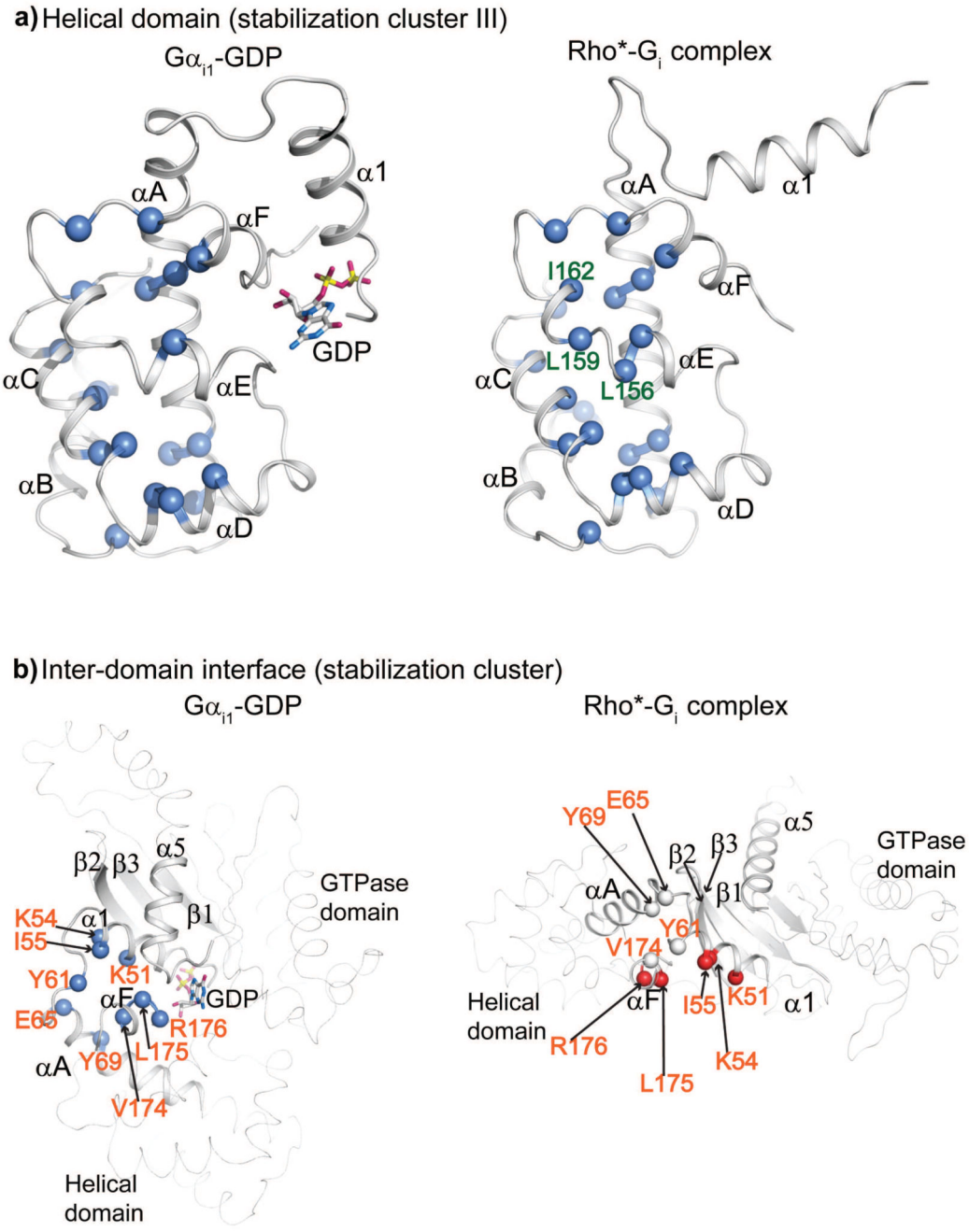

Figure 7. Close-up view of stabilization cluster III and stabilization cluster in the inter-domain interface.

a-b, Reisudes invloved in stabilization clusters in the helical domain (**a**) and inter-domain interface (**b**) in GDP-bound and receptor-bound states. The involved residues are shown as spheres in both the GDP-bound and the receptor-bound states. Light blue: destabilising effect by mutation to alanine; white: stability comparable to WT after mutation to alanine; light red: stabilization after mutation to alanine. Residues labelled in orange: alanine mutations dramatically destabilize the GDP-bound state but not the receptor-bound state;

residues labelled in forest green: alanine mutations do not affect the GDP-bound state, but significantly destabilize the receptor-bound state; residues without lableing: alanine mutation destabilize both GDP- and receptor-bound state.

Europe PMC Funders Author Manuscripts

Europe PMC Funders Author Manuscripts

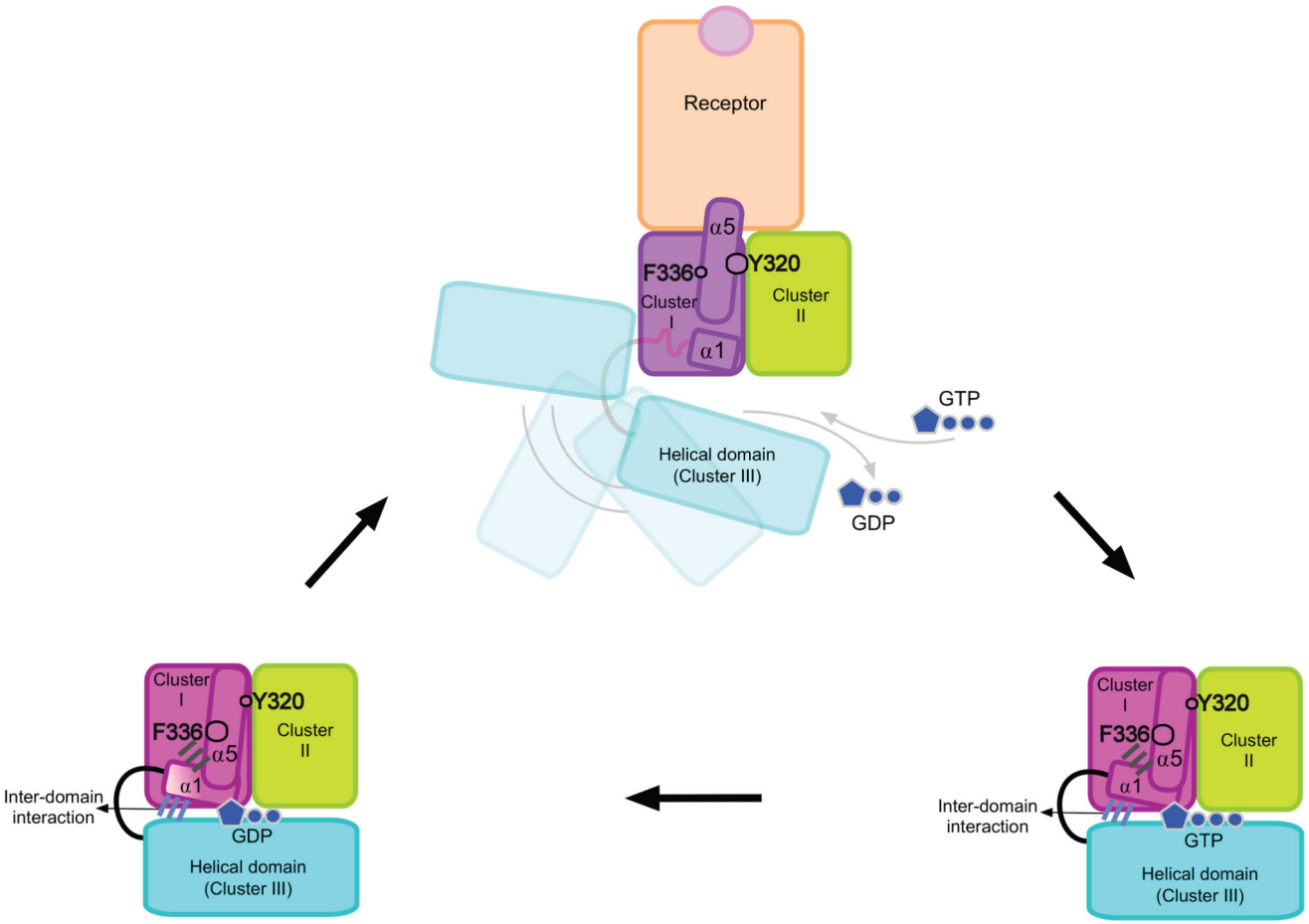

Figure 8. Nucleotide exchange in the $G\alpha_{i1}$ subunit mediated by the activation and stabilization clusters.

Cluster I is coloured in hot pink in both the GDP- and GTP-bound states, and in magenta in the receptor-bound state. Cluster II and III are coloured in lemon and cyan in the three states, respectively. The inter-domain interaction and the interactions between helices α1 and α5 are coloured in slate blue and grey, respectively. GDP and GTP are shown in dark blue. Cluster I consists of helices α1 and α5 packed against stands β1-3 in the nucleotide-bound states. In the receptor-bound state, these interactions are weakened and compensated by new interactions between helix α5 and stands β4-6. The most prominent examples of the residues involved in this rearrangement are $Y320^{G.S6.2}$, which is crucial for the stabilization of the receptor bound state, and $F336^{G.H5.8}$, important for the stability of the GDP- and GTP-bound states. Destabilization of helix α1 results in weakening of the inter-domain interface, separation of the helical domain from the GTPase domain and release of GDP.